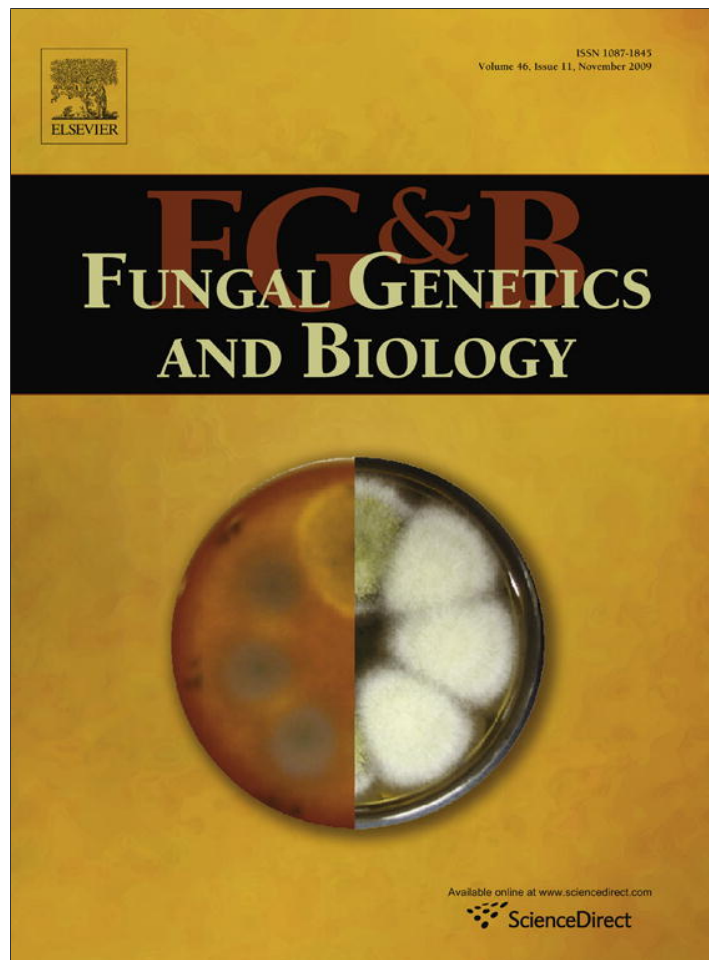


Provided for non-commercial research and education use.
Not for reproduction, distribution or commercial use.



This article appeared in a journal published by Elsevier. The attached copy is furnished to the author for internal non-commercial research and education use, including for instruction at the authors institution and sharing with colleagues.

Other uses, including reproduction and distribution, or selling or licensing copies, or posting to personal, institutional or third party websites are prohibited.

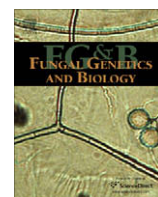
In most cases authors are permitted to post their version of the article (e.g. in Word or Tex form) to their personal website or institutional repository. Authors requiring further information regarding Elsevier's archiving and manuscript policies are encouraged to visit:

<http://www.elsevier.com/copyright>



Contents lists available at ScienceDirect

Fungal Genetics and Biology

journal homepage: www.elsevier.com/locate/yfgbi

Evolution of rDNA ITS1 and ITS2 sequences and RNA secondary structures within members of the fungal genera *Grosmannia* and *Leptographium*

Taylor Mullineux, Georg Hausner*

Department of Microbiology, University of Manitoba, Winnipeg, MB, Canada R3T 2N2

ARTICLE INFO

Article history:

Received 29 April 2009

Accepted 3 August 2009

Available online 7 August 2009

Keywords:

Ophiostomatales

ITS-rDNA

Compensatory substitutions

Strand slippage

RNA secondary structure

ABSTRACT

The two internal transcribed spacers (ITS) of the nuclear ribosomal (r) DNA tandem repeat were examined in ophiostomatoid fungi belonging to the genera *Grosmannia* and *Leptographium* and closely-related taxa. Although the DNA sequence of the ITS region evolves rapidly, core features of the RNA secondary structure of the ITS1 and ITS2 segments are conserved. The results demonstrate that structural conservation of GC-rich helical regions is facilitated primarily through compensatory base changes (CBCs), hemi-CBCs, and compensating insertions/deletions (indels), although slippage of the RNA strand is potentially an additional mechanism for maintaining basepairing interactions. The major conclusion of the structural analysis of both ITS segments is that two factors appear to be involved in limiting the type of changes observed: a high GC bias for both ITS1 and ITS2 and structural constraints at the RNA level.

© 2009 Elsevier Inc. All rights reserved.

1. Introduction

In the majority of eukaryotes the primary product of RNA polymerase I is a 35–45S rRNA precursor, composed of the 16–18S, 5.8S, and 23–28S rRNAs and the external (5' and 3' ETS) and internal (ITS1 and ITS2) transcribed spacer sequences (Good et al., 1997). The ITS1 and ITS2 segments separate, respectively, the 18S and 5.8S genes and the 5.8S and 28S genes. This precursor is processed in the nucleolus to yield the small subunit (SSU), the 5.8S, and the large subunit (LSU) rRNAs. Biochemical evidence suggests that the ITS segments are important during rRNA processing by promoting cleavage domains to be arranged in close proximity and by providing binding sites for nucleolar proteins involved in ribosome biogenesis (Nazar, 2003, 2004). Data have also shown that there is an interdependence of the ETS and ITS regions during maturation of the nucleolar rRNA precursor particle (Good et al., 1997; Lalev and Nazar, 1998, 1999, 2001; Lalev et al., 2000; Abeyrathne et al., 2002).

The ITS segments are thought to have independent origins, with ITS1 being derived from an intergenic spacer (Clark, 1987) and ITS2 from an LSU expansion segment (Nazar, 1980; Hershkovitz et al., 1999). However, in plants the two spacer regions appear to be convergent in length and substitution patterns (reviewed in Won and Renner, 2005). These observations support the suggestion that these spacers co-evolve, which is possibly due to functional constraints that maintain the reciprocal biochemical interdependence of the two ITS segments during rRNA processing.

It was previously shown that there is a positive correlation between the lengths of the ITS1 and ITS2 sequences amongst members of the Ascomycota, which is also suggestive of co-evolution of the two rDNA segments (Hausner and Wang, 2005). The latter study also showed that for this broad group of fungal genera the RNA secondary structure of the ITS segments was conserved, despite variability in the DNA sequence. Due to its wide coverage of fungal taxa and, consequently poor sequence conservation of the ITS region, the previous study was unable to identify the extent of compensatory substitutions and slippage events that may maintain the RNA secondary structure of the ITS region despite the high degree of variability in the DNA sequences. To examine this relationship, the present study focused on a narrow selection of phylogenetically related fungal species and strains that share a recent common ancestor. This reduces ambiguity in the sequence alignment and permits detailed comparative analyses for assessing the mutational dynamics of the ITS region, such as potential biases regarding GC content, expansion and contraction of the segments, CBCs (G–C to A–U, and vice versa), hemi-CBCs (G–C to G–U, and vice versa), and possible strand slippage events (Hancock and Dover, 1990).

The strains in this study belong to the anamorphic (asexual) fungal genus *Leptographium* Lagerb. & Melin and to species that have a *Leptographium* conidial state but, due to the presence of a meiotic state (telomorph), belong to the genus *Grosmannia* Goid. (Jacobs et al., 2001; Zipfel et al., 2006). The genus *Grosmannia* belongs to the order *Ophiostomatales* (Ascomycota) (Hibbett et al., 2007). Typically members of the genus *Leptographium* are phylogenetically allied to members of *Grosmannia*, and like many other ophiostomatoid fungi they are associated with bark beetles that

* Corresponding author. Fax: +1 204 474 7603.

E-mail address: hausnerg@cc.umanitoba.ca (G. Hausner).

can vector these fungi to new plant hosts/sites. In many areas *Leptographium* species are becoming increasingly problematic as new species are introduced due to the arrival or introduction of new bark beetle species that serve as potential vectors (Hausner et al., 2005). These fungi are of particular interest to the forestry industry, as they are blue-stain fungi that can reduce the value of stored lumber and some species are serious plant pathogens (Harrington, 1993).

In addition to their use as a marker for phylogenetic studies, ITS sequences are utilized in the identification of fungal species, such as in culture-independent, high-throughput automated approaches for the characterization of fungal communities from various habitats (Ranjard et al., 2001; Horton, 2002; Buchan et al., 2002; Kennedy and Clipson, 2003; Druzhinina et al., 2005; Mitchell and Zuccaro, 2006; Nilsson et al., 2009). In the case of pathogenic organisms, sequence analysis of ITS regions may be useful in the identification of native or exotic plant pathogens (Hausner et al., 2005; Zhang et al., 2008).

The goals of the current study are twofold: firstly, to identify mechanisms involved in conserving RNA secondary structure in spite of the rapid evolution of the DNA sequence and secondly, to assess both the level of branch support and the effects on tree topology obtained from the phylogenetic analysis of each segment individually and of the entire ITS1-5.8S-ITS2 region. To address the first issue we used comparative sequence analysis to develop models of RNA secondary structure and to identify the potential effects of CBCs, hemi-CBCs, and indels on secondary structure. This may assist in generating improved structure-guided DNA sequence alignments of rapidly evolving regions, including ITS. This approach takes advantage of conserved features of secondary structures to facilitate the alignment of ambiguous regions and as such may be useful for analyses based on ITS sequences, especially given the wide-spread application of this region as a marker in phylogenetic and fungal barcoding studies. To examine the second issue, we carried out phylogenetic analyses on the entire ITS-5.8S rDNA region and each ITS segment individually.

2. Materials and methods

2.1. DNA extraction and the amplification and sequencing of ITS1-5.8S-ITS2 nuclear rDNA

The maintenance of fungal cultures and DNA extraction protocols employed in the present study are described in Hausner et al. (1992). The strains used in this study are listed in Table 1. The ITS1-5.8S-ITS2 region was amplified by PCR using the 1.5X PCR Enhancer System (Invitrogen Canada Inc., Burlington, Canada), containing ($\mu\text{L}/\text{reaction}$): 10X PCR \times amplification buffer (5); 2.5 mM dNTP (4); 50 mM MgSO_4 (1.5); 40 μM each of forward and reverse primers (0.5 + 0.5); 10X PCR \times enhancer solution (7.5); Taq polymerase (0.25), sterile Milli-Q water (29.75); and genomic DNA template (1). The oligonucleotide primers used for amplification, SSZ, LS4, SS3, and LS2, have been described elsewhere (Hausner et al., 1993a; Hausner and Wang, 2005). Amplification was carried out using the following standard conditions: initial denaturation (93 °C, 2 min), denaturation (93 °C, 1 min), primer annealing (50 °C, 1 min), extension (72 °C, 1 min), 30 cycles. When necessary, the temperature and length of the annealing and/or extension steps, template concentration, and the number of cycles were optimized to obtain single, sharp bands. PCR products were purified using the Wizard[®] SV Gel and PCR Clean-Up System (Promega Corp., Madison, USA) and eluted in a final volume of 35–50 μL of nuclease-free water.

The cycle-sequencing of PCR products was done according to the Big Dye (version 3.1) protocols supplied by the manufacturer

(Applied Biosystems, Foster City, USA). The resulting sequencing products were purified and resolved on an automated fluorescent DNA sequence analysis system using an Applied Biosystems 3730XL 96 capillary sequencer (Applied Biosystems).

Sequence data were obtained from GenBank and from strains housed at the WIN(M) herbarium (University of Manitoba). Identical sequences were identified using DAMBE (Xia, 2000) and discarded for this study, leaving datasets of 70 (ITS-5.8S region), 55 (ITS1), and 46 (ITS2) unique sequences.

2.2. Analyses of DNA sequence data

ITS sequences were aligned manually using GeneDoc V2.7.000 (Nicholas et al., 1997). Programs contained within PAUP^{*} version 4.0b10 (Swofford, 2002), PHYLIP Version 3.68 (Felsenstein, 2008), MrBayes v3.1.2 (Ronquist and Huelsenbeck, 2003), Tree-Puzzle version 5.2 (Schmidt et al., 2002), and the Willi Hennig Society edition of TNT (Goloboff et al., 2008) were utilized for phylogenetic analyses. *Ceratocystis deltoideospora* strain WIN(M)41 was selected as the outgroup for all phylogenetic analyses, although *Ceratocystiopsis collifera* strain CBS126.89 was included as a second outgroup (Zipfel et al., 2006). For maximum parsimony phylogenetic estimates were evaluated using the bootstrap procedure (SEQBOOT: 1000 replicates, jumble three times) and CONSENSE in PHYLIP. For Bayesian analysis, Modeltest 3.7 (Posada and Crandall, 1998) was used to select models of evolution. Based on the Akaike Information Criterion (AIC), the TVM+I+G model was selected for analysis of the ITS-5.8S region and ITS1, while ITS2 was analyzed with the TVM+G model. In all cases we allowed the parameters to be estimated by MrBayes. The analyses were run for 15 million generations and the sampling frequency was set to 1000. To generate 50% majority rule consensus trees with posterior probability values 50% of the trees were discarded. Analysis with the Tree-Puzzle program (maximum likelihood phylogenetic analysis using quartets and parallel computing) used the following settings for the quartet puzzling algorithms: 25,000 puzzling steps; transition/transversion parameter estimated from the datasets; and HKY evolutionary model (Hasegawa et al., 1985). The topology of the tree obtained from TNT confirmed the topology of the trees obtained using PHYLIP and were not included in this study. The phylogenetic trees presented were drawn with the Tree View program version 1.6.6 (Page, 1996) using the Bayesian consensus outfile and annotations were added to the figure using CoreIDRAW version 14 (Ottawa, Canada). Data relevant to the phylogenetic analysis were deposited in TreeBase under the following accession numbers: S2443 (Study accession number), M4645 (Matrix accession number), and M4646 (Matrix accession number).

2.3. Sequence and structural analyses

The Weblogo program (Crooks et al., 2004) was used to generate sequence logos (Schneider and Stephens, 1990) for assessing both sequence conservation within ITS1 and ITS2 and the relative frequency of the nucleotides at each position. To generate the sequence logos the sequences for the phylogenetic outgroups were removed from the alignment.

Models of RNA secondary structure of ITS1 and ITS2 were developed using Mfold (Mathews et al., 1999; Zuker, 2003) and the number of constraints (either forcing or prohibiting base pairing interactions) was kept to a minimum. For ITS1, motifs common to the majority of strains, such as the loops/helices near the 5' and 3' termini and features within the major helix, were identified. Structural models for the remaining strains were determined based on comparative sequence analysis using these features as a guide. Proposed models for ITS2 were compared to those available in the ITS2 Database II (Selig et al., 2008). Our proposed models

Table 1Strains of *Grosmannia*, *Leptographium*, and related taxa used in this study, along with GenBank accession numbers.

Strain ^a	Accession number	Strain	Accession number	Strain	Accession number
<i>Ceratocystiopsis collifera</i> CBS126.89	EU913721	<i>Leptographium</i> sp. J.R.88–194A	AY935622	<i>L. terebrantis</i> UAMH9722	AY935605
<i>Ceratocystis deltoideospora</i> ^b WIN(M)41	EU879121	<i>Leptographium</i> sp. WIN(M)528	EU879138	<i>L. truncatum</i> CBS929.85	AY935626
<i>Grosmannia aurea</i> CBS438.69	AY935605	<i>Leptographium</i> sp. WIN(M)984	EU879122	<i>L. truncatum</i> NFR1813/1	AY935591
<i>G. cucullata</i> C1216	AF198246	<i>Leptographium</i> sp. WIN(M)985	EU879123	<i>L. truncatum</i> TOM74.29	AY935581
<i>G. davidsonii</i> WIN(M)60B	EU879127	<i>Leptographium</i> sp. WIN(M)1106	EU879147	<i>L. truncatum</i> TOM86.30	AY935582
<i>G. davidsonii</i> WIN(M)1132	EU879129	<i>Leptographium</i> sp. WIN(M)1247	EU879146	<i>L. serpens</i> WIN(M)1214	EU879144
<i>G. davidsonii</i> WIN(M)1494	EU879126	<i>Leptographium</i> sp. WIN(M)1269	EU879145	<i>L. wingfieldii</i> CBS645.89	AY935603
<i>G. davidsonii</i> WIN(M)1495	EU879134	<i>L. americanum</i> WIN(M)1456	EU879139	<i>L. wingfieldii</i> CBS648.89	AY935611
<i>G. dryocoetes</i> CBS376.66	AJ538340	<i>L. lundbergii</i> CBS352.29	AY935585	<i>L. wingfieldii</i> MCC125	AY935608
<i>G. europhoides</i> CBS229.83	EU879141	<i>L. lundbergii</i> DAOM64746	EU879151	<i>L. wingfieldii</i> MCC130	AY935612
<i>G. europhoides</i> MUCL18355	AJ538333	<i>L. lundbergii</i> DSMZ5010	AY935589	<i>L. wingfieldii</i> MCC349	AY935610
<i>G. europhoides</i> NFR180–67/22	EU879140	<i>L. lundbergii</i> NFR160–25	AY925584	<i>L. wingfieldii</i> TOM10.2	AY935599
<i>G. francke-grosmanniae</i> ATCC22061	EU879125	<i>L. lundbergii</i> NFR169–148	AY935588	<i>L. wingfieldii</i> TOM11.5	AY935602
<i>G. galeiformis</i> C1101	DQ062679	<i>L. lundbergii</i> NFR189–1040/1/3	AY935586	<i>L. wingfieldii</i> TOM59.21	AY935600
<i>G. galeiformis</i> CECT 20482	AJ538334	<i>L. procerum</i> DAOM33940	AY935613	<i>L. wingfieldii</i> WIN(M)1218	EU879152
<i>G. huntii</i> WIN(M)492	EU879148	<i>L. procerum</i> NFR159–84/2	AY935618	<i>L. wingfieldii</i> WIN(M)1322	EU879154
<i>G. laricis</i> CBS636.94	AJ538332	<i>L. procerum</i> TOM73.12	AY935615	<i>L. wingfieldii</i> WIN(M)1382	EU879153
<i>G. penicillata</i> NFR160–21	AY935623	<i>L. procerum</i> TOM76.8	AY935614	<i>L. wingfieldii</i> WIN(M)1482	EU879155
<i>G. penicillata</i> WIN(M)131	EU879137	<i>L. procerum</i> WIN(M)1264	EU879143	<i>O. brevicolle</i> ^b CBS150.78	EU879124
<i>G. piceaperda</i> WIN(M)980	EU978150	<i>L. terebrantis</i> CBS298.85	AY935598	<i>Pesotum</i> sp. WIN(M)478	EU879130
<i>G. piceaperda</i> WIN(M)1380	EU879149	<i>L. terebrantis</i> CBS337.70	AY935609	<i>Pesotum</i> sp. WIN(M)481	EU879133
<i>G. pseudoeurophoides</i> WIN(M)42	EU879136	<i>L. terebrantis</i> CBS408.61	AY935597	<i>Pesotum</i> sp. WIN(M)1423	EU879128
<i>G. wagneri</i> ATCC58579	AY935596	<i>L. terebrantis</i> UAMH9690	AY935607	<i>Pesotum</i> sp. WIN(M)1428	EU879131
<i>Hyalopesotum pini</i> WIN(M)82–89	EU879132				

^a J.R., J. Reid; CBS, Central Bureau voor Schimmelcultures, Utrecht, The Netherlands; WIN(M), University of Manitoba, Microbiology/Botany (J.R.'s personal collection); UAMH, University of Alberta Microfungus Collection and Herbarium, Devonian Botanic Garden, Edmonton, AB, Canada, T 6G 2E1; ATCC, American Type Culture Collection, Rockville, MD, USA; NFR1, Norwegian Forest Research Institute, AS, Norway; DAOM, Cereal and Oilseeds Research, Agriculture & Agri-Food Canada, Ottawa, Ont., Canada; culture collection of H. Masuya; TOM, Isolation designation, Canadian Forest Service, Great Lakes Forestry Centre, 1219 Queen St., Sault Ste. Marie, ON, P6A 5M7.

^b *Ceratocystis deltoideospora* is a species that should be transferred to *Ophistoma* (Hausner et al., 1993b); and *Ophistoma brevicolle* is a species that should be transferred to *Grosmannia* (Zipfel et al., 2006).

conformed to those in the database. Structures were modeled using conserved sequence/structural features in helices I–IV as a template.

To generate RNA structure logos (Gorodkin et al., 1997) for each ITS segment the two phylogenetic outgroups were removed from the sequence alignment. *Pesotum* sp. strain WIN(M)481, a strain that is distantly related to the remaining strains in the study, was used as the reference in this alignment: RNA structural models of each ITS segment for this strain were converted to Vienna notation (in which brackets indicate base pairing and dots represent unpaired nucleotides) in Mfold (Mathews et al., 1999; Zuker, 2003; Meyer and Miklós, 2007) and the text file containing the Vienna notation of *Pesotum* sp. strain WIN(M)481 and the DNA sequence of the remaining strains was uploaded to the RNA structure logo site (<http://www.cbs.dtu.dk/~gorodkin/appl/slogo.html>). Logos were generated using the default parameters: type two logo, *a priori* nucleotide distribution probability of 0.25 for each of the four ribonucleotides and a base pair weight probability of 1.0 for AU, CG, and GU base pairs. The logos were examined for “mutual information” (Gorodkin et al., 1997), that is, sites where there is base pairing in the absence of nucleotide conservation.

3. Results

3.1. Characteristics of the ITS region in *Leptographium* and related taxa

The data set contained 70 sequences for the ITS region (Table 1). Amongst these 70 sequences, 55 had unique ITS1 sequences and only 46 had unique ITS2 sequences. The lengths and GC contents of ITS1, ITS2, and the 5.8S gene for the strains used in this study are described in Table 2. The size of the ITS1 and ITS2 segments range, respectively, from 157 to 232 nt (mean, 202 nt) and 177 to 233 nt (mean, 197 nt). The ITS regions are GC-rich: mol% GC values range from 54.4 to 69.6 (mean, 65.3) in the ITS1 segment and 63.5

to 77.9 (mean, 72.3) in ITS2. The GC content of the 5.8S gene is considerably lower, ranging from 48.4% to 50.6% (mean 49.9%).

3.2. Characterizing the DNA sequence of ITS1 and ITS2 with DNA sequence logos

DNA sequence logos (Figs. 1a and 2a) were constructed for both ITS segments in order to easily visualize conserved regions and local sequence biases, such as expansion or contraction segments and mono and di-nucleotide repeats. Within ITS1 there are two GC-rich regions within the hairpin that are potential hotspots for compensatory changes, including nucleotide substitutions and indels; the latter are responsible for the expansion or contraction of the length of the hairpin (Fig. 1b). These basepairing interactions may be formed between nucleotides that are separated by a great distance: the segment near the 5' terminus, which is dominated by GA repeats (positions 58–68, as numbered in Fig. 1a), forms an extended hairpin with a downstream C/CT rich sequence (positions 199–207). Near the terminus of the helix (Fig. 1b), the 5' CT stretch (positions 100–117) forms a hairpin with a series of Gs on the 3' side (positions 123–142) of the stem. Comparing the sequence logo with the original sequence alignment reveals sites of potential replication slippage, which we have defined as sites at which the sequence for one or two strains contains a stretch of the same base or a repeat of a short nucleotide pattern that is not found in the remaining strains. Putative replication slippage was identified in *G. piceaperda* strain WIN(M)1380: within a GC-rich stretch there is an insert of CGG (positions 188–190), followed by a stretch of Gs (see Fig. 1a, positions 209–212). There are helical-loop regions near the termini of ITS1 in which the nucleotides are highly conserved. These regions are part of the central helix, which previous biochemical studies have shown is involved in forming a complex with soluble protein factors involved in rRNA maturation/ribosome biogenesis (Lalev and Nazar, 1999).

Table 2
Nucleotide composition and GC content of nuclear ITS1 and ITS2 sequences in strains of *Grosmannia*, *Leptographium*, and related taxa.

Strain	ITS1				ITS2				5.8S rDNA					
	Length (nt)	%GC	A	T	G	C	Length (nt)	%GC	A	T	G	C	Length (nt)	%GC
Outgroup ^a														
<i>Ceratocystis deltoideospora</i> WIN(M)41	202	68.3	29	35	57	81	190	77.9	22	20	66	82	159	49.1
<i>Ceratocystiopsis collifera</i> CBS126.89	160	54.4	40	33	32	55	181	71.3	23	29	54	75	159	49.1
Clade I ^b														
<i>Hyalopesotum pini</i> WIN(M)82–89	158	69.6	26	22	45	65	185	76.8	22	21	61	81	159	50.3
<i>Grosmannia galeiformis</i> C1101	158	69.6	26	22	45	65	185	76.8	22	21	62	80	159	50.3
<i>G. galeiformis</i> CECT 20482	157	69.4	26	22	45	64	185	76.8	22	21	61	81	159	50.3
Minimum–maximum (mean)	157–158 (158)	69.4–69.6 (69.5)												
Clade II														
<i>G. cucullata</i> C1216	174	63.8	30	33	50	61	194	67.0	27	37	60	70	159	49.7
<i>G. davidsonii</i> WIN(M)60B	175	62.9	31	34	50	60	194	66.0	27	39	60	68	159	49.7
<i>G. davidsonii</i> WIN(M)1132	175	62.9	31	34	50	60	194	66.5	27	38	60	68	159	49.7
<i>G. davidsonii</i> WIN(M)1494	174	63.2	31	33	50	60	194	66.5	27	38	60	68	159	49.7
<i>G. francke-grosmanniae</i> ATCC22061	173	63.6	32	31	47	63	192	66.7	26	38	66	62	159	49.7
<i>Ophiotoma brevicolle</i> CBS150.78	171	59.1	33	37	47	54	192	63.5	30	40	58	64	159	50.3
<i>Pesotum</i> sp. WIN(M)478	174	62.6	31	34	50	59	194	66.5	27	38	60	69	159	49.7
<i>Pesotum</i> sp. WIN(M)1423	174	62.6	31	34	50	59	194	67.0	27	37	60	70	159	49.7
<i>Pesotum</i> sp. WIN(M)1428	174	63.2	30	34	51	59	194	66.5	27	38	60	70	159	49.7
Minimum–maximum (mean)	171–175 (174)	59.1–63.8 (62.7)					192–194 (194)	63.5–67.0 (66.2)						49.7–50.3 (49.8)
Clade III														
<i>G. dryocoetis</i> CBS376.66	179	65.4	30	32	48	69	185	70.3	28	27	60	70	159	48.4
<i>G. pseudoeurophioides</i> WIN(M)42	177	65.5	29	32	50	66	188	69.1	30	28	59	71	159	48.4
<i>Leptographium</i> sp. J.R.88–194A	177	63.8	31	33	49	64	201	75.1	23	27	64	87	159	50.3
<i>Leptographium</i> sp. WIN(M)528	177	66.1	29	31	50	67	187	65.8	34	30	68	55	159	48.4
<i>L. americanum</i> WIN(M)1456	177	66.7	29	30	50	68	188	66.5	33	30	56	69	159	48.4
<i>G. penicillata</i> NFR160-21	178	63.5	31	33	48	65	187	68.4	31	28	58	70	159	48.4
<i>G. penicillata</i> WIN(M)131	177	63.8	31	33	49	64	187	67.4	31	30	57	69	159	48.4
Minimum–maximum (mean)	177–179 (177)	63.5–66.7 (65.0)					185–201 (189)	65.8–75.1 (68.9)						48.4–50.3 (48.7)
Clade IV														
<i>G. huntii</i> WIN(M)492	216	65.7	30	44	63	79	199	74.4	23	28	63	85	159	50.3
<i>G. piceaperda</i> WIN(M)980	214	66.4	30	42	60	82	203	75.9	22	27	64	90	159	50.3
<i>G. piceaperda</i> WIN(M)1380	232	66.8	34	43	69	86	233	75.1	25	33	77	98	159	50.3
Minimum–maximum (mean)	214–232 (221)	65.7–66.8 (66.3)					199–233 (212)	74.4–75.9 (75.1)						
Clade Va														
<i>G. aurea</i> CBS438.68	221	65.2	32	45	65	79	200	74.0	24	28	64	84	159	50.3
<i>L. terebrantis</i> CBS298.85	227	65.2	34	45	66	82	200	74.0	24	28	64	84	159	50.3
<i>L. terebrantis</i> CBS337.70	226	65.5	33	45	66	82	200	74.0	24	28	64	84	159	50.3
<i>L. terebrantis</i> CBS408.61	220	64.5	32	46	64	78	200	74.0	24	28	64	84	159	50.3
<i>L. terebrantis</i> UAMH9690	222	65.3	33	44	64	81	200	74.5	24	27	64	85	159	50.3
<i>L. terebrantis</i> UAMH9722	221	65.2	32	45	65	79	200	73.5	25	28	64	83	159	50.3
<i>L. wingfieldii</i> CBS645.89	220	65.0	32	45	64	79	200	74.0	24	28	64	84	159	50.3
<i>L. wingfieldii</i> CBS648.89	220	65.0	32	45	64	79	201	74.1	24	28	64	85	160	50.6
<i>L. wingfieldii</i> MCC125	224	66.1	32	44	67	81	200	74.5	24	27	64	85	159	50.3
<i>L. wingfieldii</i> MCC130	223	65.5	33	44	64	82	200	74.0	24	28	64	84	159	48.4
<i>L. wingfieldii</i> MCC349	220	65.0	32	45	64	79	200	74.0	24	28	64	84	156	49.4
<i>L. wingfieldii</i> TOM10.2	217	64.5	32	45	61	79	200	74.0	24	28	64	84	159	50.3
<i>L. wingfieldii</i> TOM11.5	217	64.5	32	45	61	79	200	74.0	24	28	63	85	159	50.3
<i>L. wingfieldii</i> TOM59.21	217	64.5	32	45	61	79	200	73.5	25	28	63	84	159	50.3
<i>L. wingfieldii</i> WIN(M)1218	225	65.3	33	45	65	82	200	74.0	24	28	64	84	159	50.3
<i>L. wingfieldii</i> WIN(M)1322	223	65.9	32	44	66	81	200	73.5	24	29	64	83	159	50.3
<i>L. wingfieldii</i> WIN(M)1382	222	65.3	33	44	64	81	200	74.5	24	27	64	85	159	50.3
<i>L. wingfieldii</i> WIN(M)1482	222	65.3	32	45	66	79	200	74.0	24	28	64	84	159	50.3
Minimum–maximum (mean)	217–227 (221)	64.5–66.1 (65.2)					200–201 (200)	73.5–74.5 (74.0)					156–160 (159)	48.4–50.6 (50.2)
Clade Vb														
<i>L. lundbergii</i> CBS352.29	218	67.9	33	37	63	85	199	74.9	23	27	63	86	159	50.3
<i>L. lundbergii</i> DAOM64746	223	64.1	36	44	63	80	200	74.0	23	29	63	85	159	50.3
<i>L. lundbergii</i> DSMZ5010	218	67.9	33	37	63	85	198	74.7	23	27	62	86	159	50.3
<i>L. lundbergii</i> NFR160-25	217	68.2	33	36	63	85	199	74.9	23	27	63	86	159	50.3
<i>L. lundbergii</i> NFR169-148	218	67.9	33	37	63	85	200	74.0	24	28	62	86	159	49.7
<i>L. lundbergii</i> NFR189-1040/1/3	218	67.9	33	37	63	85	199	74.4	24	27	63	85	159	50.3

Table 2 (continued)

Strain	ITS1				ITS2				5.8S rDNA					
	Length (nt)	%GC	A	T	G	C	Length (nt)	%GC	A	T	G	C	Length (nt)	%GC
Minimum–maximum (mean)	217–223 (219)	64.1–68.2 (67.3)					198–200 (199)	74.0–74.9 (74.5)						49.7–50.3 (50.2)
Clade Vc														
<i>Leptographium</i> sp. WIN(M)1106	219	68.5	31	38	63	87	200	74.5	23	28	63	86	159	50.3
<i>Leptographium</i> sp. WIN(M)1247	215	67.4	31	39	63	82	200	74.5	23	28	63	86	159	50.3
<i>Leptographium</i> sp. WIN(M)1269	219	68.5	30	39	65	85	200	74.5	23	28	63	86	159	50.3
<i>L. truncatum</i> CBS929.85	214	68.7	30	37	63	84	200	75.5	23	26	64	87	159	50.3
<i>L. truncatum</i> NFRI18–13/1	215	68.8	30	37	63	85	200	75.5	23	26	64	87	159	50.3
<i>L. truncatum</i> TOM74.29	215	68.8	30	37	63	85	200	75.5	23	26	64	87	159	50.3
<i>L. truncatum</i> TOM86.30	215	67.9	31	38	63	83	200	74.5	23	28	63	86	159	50.3
Minimum–maximum (mean)	214–219 (216)	67.4–68.8 (68.4)						74.5–75.5 (74.9)						
Clade VI														
<i>Leptographium</i> sp. WIN(M)984	196	64.8	35	34	56	71	209	68.4	31	35	63	80	159	49.7
<i>Leptographium</i> sp. WIN(M)985	196	64.8	35	34	56	71	210	68.1	31	36	63	80	159	49.7
Clade VII														
<i>G. europhioides</i> CBS229.83	224	61.2	40	47	61	76	200	69.5	23	38	62	77	159	50.3
<i>G. europhioides</i> MUCL18355	222	59.9	41	48	58	75	200	70.5	23	36	62	79	159	50.3
<i>G. europhioides</i> NFRI80–67/22	224	61.2	40	47	61	76	199	69.8	23	37	62	77	159	50.3
<i>G. laricis</i> CBS636.94	223	60.5	40	48	60	75	200	70.0	23	37	62	78	159	50.3
Minimum–maximum (mean)	222–224 (223)	59.9–61.2 (60.7)					199–200 (200)	69.5–70.5 (69.9)						
Clade VIII														
<i>G. wagneri</i> ATCC58579	202	67.3	31	35	56	80	198	73.7	25	27	64	82	159	50.3
<i>L. serpens</i> DAOM173660	206	68.4	28	37	59	82	198	73.2	26	27	64	81	159	49.7
Clade IX														
<i>L. procerum</i> DAOM33940	174	64.4	28	34	44	68	203	71.9	26	31	63	83	159	50.3
<i>L. procerum</i> NFRI59–84/2	184	63.6	30	37	49	68	203	71.9	26	31	63	83	159	50.3
<i>L. procerum</i> TOM73.12	207	67.1	30	38	60	79	203	71.9	26	31	63	83	159	50.3
<i>L. procerum</i> TOM76.8	207	67.1	30	38	60	79	203	71.9	26	31	63	83	159	50.3
<i>L. procerum</i> WIN(M)1264	207	67.1	30	38	61	78	203	71.9	26	31	63	83	159	50.3
Minimum–maximum (mean)	174–207 (196)	63.6–67.1 (65.9)												
Clade X														
<i>G. davidsonii</i> WIN(M)1495	171	66.1	27	31	49	64	177	75.7	25	18	59	75	159	49.1
<i>Pesotum</i> sp. WIN(M)481	171	66.1	27	31	49	64	177	75.7	25	18	60	74	159	49.1

^a The strains used as the phylogenetic outgroups as shown in Fig. 3.

^b Clades are described in Fig. 3.

In ITS2 the 5' terminus is invariant (Fig. 2a): the 3' terminus of the 5.8S gene and the first three nucleotides of ITS2 form a hairpin with the 5' terminus of the LSU (Fig. 2b). An earlier investigation of the core secondary structure of ITS2 in green algae and flowering plants found the sequence and length of helix I to be variable (Mai and Coleman, 1997). In contrast, in strains of *Leptographium* and *Grosmanina* the terminal loop was variable, while the stem region exhibited little variation in length or sequence. Further, in *G. piceaperda* strain WIN(M)1380 there is evidence suggestive of replication slippage in helix I (Fig. 2a and b; positions 29–31). Helix II is less conserved, particularly in the terminal loop. There are numerous inserts as well as sites of putative replication slippage in helix II: the stretch of Gs (positions 103–110) observed in *G. piceaperda* strain WIN(M)1380 represents one such example. The 3' terminus at the base of helix III is hyper variable and is one of the main sites of potential RNA strand slippage. Helix IV is variable in length and sequence; this variation is potentially influenced by RNA strand slippage events occurring in helix III and in the single-stranded “palm” region between helices III and IV.

3.3. Models of RNA secondary structure of ITS1 and ITS2

Models of RNA secondary structure were generated for ITS1 and ITS2 (Figs. 1b and 2b). For the ITS1 region an extended hairpin structure that lacked any side helices was identified, as well as several conserved loops and shorter helices (Fig. 1b). This “core”

structure was subsequently used as a template to guide the folding of ITS1 sequences for more distantly related taxa using comparative sequence analysis, which involves the identification of CBCs to support proposed base pairing interactions. One exception to this model occurs in the RNA structure for *L. procerum* strain NFRI59–84/2, which contains a small lateral helix on the 5' side of the hairpin as a result of a large deletion on the 3' side of the helix that disrupts base pairing with opposing nucleotides on the 5' side. Alternative structures containing small side helices, as described by Nazar et al. (1987), were obtained, indicating that in these GC-rich segments alternative interactions between bases on opposing sides of the hairpin are possible. Flexibility in base pairing is especially relevant in RNA due to GU “wobble” interactions. RNA structural models of ITS2 (Fig. 2b) conform to the previously proposed ITS2 “core” secondary structural model: a model of four helices radiating from a central loop, with helix III as the longest hairpin (Coleman, 2007; Keller et al., 2009), as shown in Fig. 2b. This model has been examined using functional genetic assays (Côté et al., 2002).

3.4. Evolution of the ITS region

Phylogenetic analyses were carried out on the ITS1–5.8S–ITS2 region and on each segment individually for the purpose of: (1) examining the evolution of DNA sequence and RNA secondary structure amongst closely-related sequences; (2) determining if

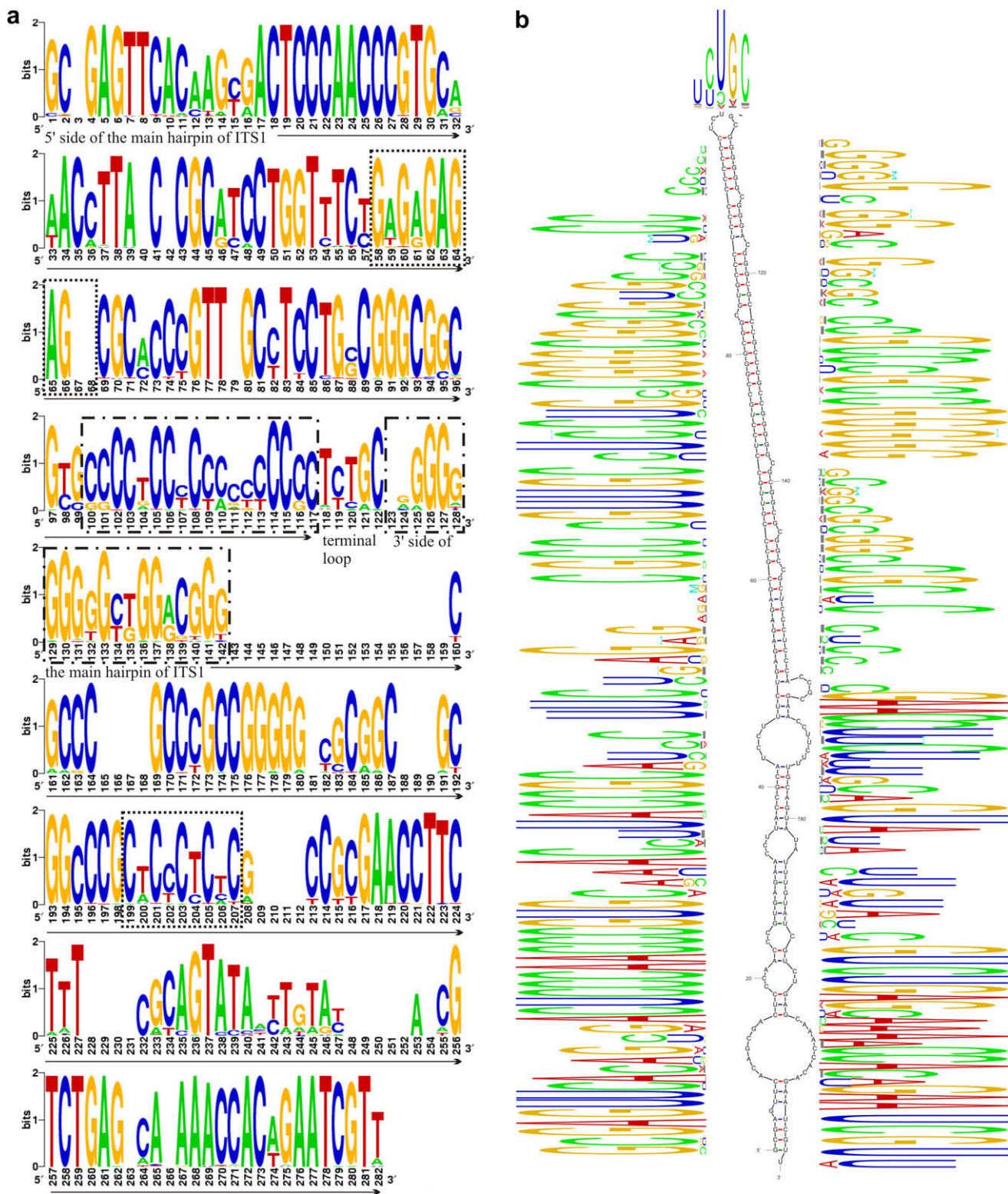


Fig. 1. DNA weblogo of the ITS1 segment in strains of *Grossmannia*, *Leptographium*, and related taxa. (a) Regions representing potential tandem repeats or expansion/contraction segments are enclosed in boxes. Model of the RNA secondary structure of the ITS1 segment of *L. truncatum* strain TOM86.30. (b) The RNA structure logo is mapped onto the model. The proposed model suggests that nucleotides found in the series of loops and short hairpins near the 5' and 3' termini are highly conserved.

observed sequence and structural features are conserved across taxa or are unique to a particular clade; and (3) assessing branch support and tree topology obtained from the entire region versus the ITS1 or ITS2 segments (Fig. 3, Supplementary Figs. 1 and 2). The analysis revealed taxonomic novelties with respect to *G. davidsonii* that will be addressed in a future study. Amongst the

fungi treated in this study ITS1 sequences are noted to be less conserved than ITS2 sequences. This has been observed in other fungal taxa (Goertzen et al., 2003; Schultz et al., 2005; Wolf et al., 2005; Piercey-Normore et al., 2006), but it has been noted recently that there are many examples within the fungi in which the ITS2 segment is more variable (Nilsson et al., 2008). Overall, within our

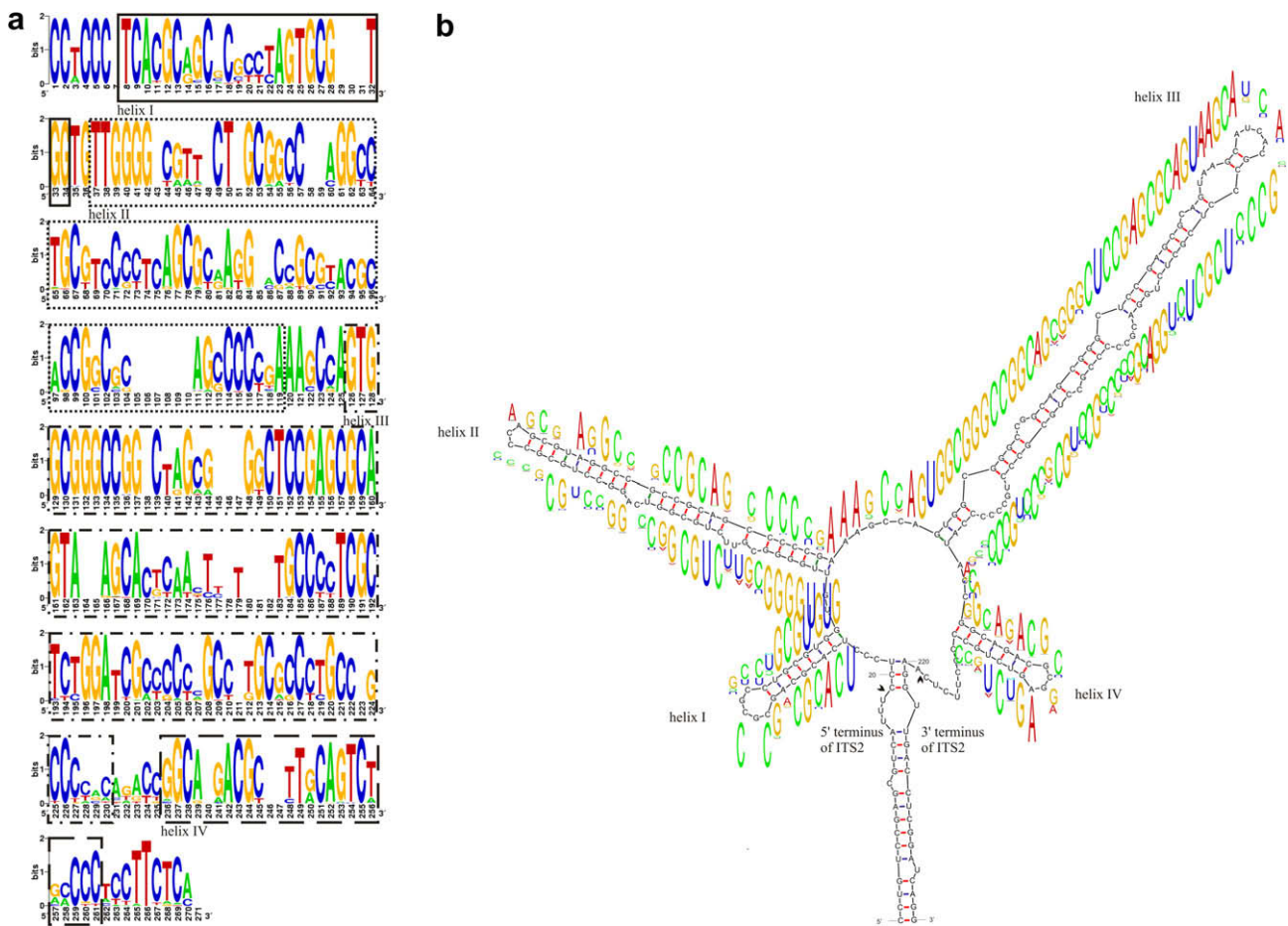


Fig. 2. DNA weblogo of the ITS2 region in strains of *Grossmannia*, *Leptographium*, and related taxa. (a) Helices I–IV are enclosed in boxes. Model of the RNA secondary structure of the ITS2 segment of *L. truncatum* strain TOM86.30. (b) The RNA structure logo is mapped onto the model. The model conforms to the pan-eukaryotic “four-fingered hand model” proposed by Coleman (2007). Nucleotides at the 5' terminus are conserved and base pair with the 5' terminus of the LSU.

data set we observed a greater variability in the size of the ITS1 segment compared to that of ITS2. The ITS1 segment was also more variable in sequence than ITS2: of the 70 strains in the data set, there were 55 unique ITS1 sequences and only 46 unique ITS2 sequences. Furthermore, amongst closely-related strains of ophiostomatoid fungi the ITS region is less variable, but between more distantly related taxa there was increased sequence ambiguity in the variable regions of the ITS segments.

We have identified 10 major clades in the Bayesian tree obtained from analysis of the ITS-5.8S region (Fig. 3). Clade V has been further subdivided into three subclades, comprised of strains of *L. wingfieldii*-*L. terebrantis*-*G. aurea* species complex (clade Va), *L. lundbergii* (clade Vb), and *L. truncatum* (clade Vc). As suggested by the topology of the tree and its branch lengths ITS variability is more pronounced between the clades rather than within the species examined in this study. The ITS1 segment exhibits the greatest variability in length and GC content in the *L. wingfieldii*-*L. terebrantis*-*G. aurea* species complex compared to the other subclades. Two strains of *L. terebrantis* CBS298.85 and *L. terebrantis* CBS337.70 are remarkable for having numerous insertions in the ITS1 region, yet their ITS2 sequence is identical to each other and to *L. wingfieldii* strain WIN(M)1218 (Supplementary Figs. 1 and 2). Diversity in the ITS region amongst strains belonging to clade IV is the result of numerous insertions and potential replication slippage events observed in *G. piceaperda* strain WIN(M)1380 (Fig. 1a). Members of clade IX exhibit the greatest variation in the ITS1 segment. *Leptographium procerum* strains NFR159-84/2 and DAOM33940 have unusually short ITS1 sequences of 184

and 174 nt, respectively, as a result of large deletions in GC-rich regions on the 3' side of the hairpin.

In contrast to the variability observed in the size of ITS1 segment, there is little variation in the size of the ITS2 region, even in those strains with reduced ITS1 segments (Table 2, Fig. 3). In *Pesotum* sp. strain WIN(M)481 and *G. davidsonii* strain WIN(M)1495 the ITS segments are similar in size: ITS1 and ITS2 are, respectively, 171 nt and 177 nt in length. In strain *G. piceaperda* strain WIN(M)1380 both segments are greater in length (232 nt and 233 nt for ITS1 and ITS2, respectively) than the average size for the other two members of clade IV (average is 221 nt and 212 nt for ITS1 and ITS2, respectively); the increase in size is due to possible replication slippage (Figs. 1 and 2).

Polytomies in the phylogenetic tree were reduced when the phylogenetic analysis incorporated the entire ITS-5.8S region rather than either segment on its own (compare Fig. 3 with Supplementary Figs. 1 and 2). When ITS2 in particular is used as the phylogenetic marker species distinction and branch support are significantly reduced and several clades are reduced to polytomies (Fig. 3, Supplementary Figs. 1 and 2). This is especially evident with members of clade IX: all five strains of *L. procerum* share identical ITS2 segments but are differentiated from each other based on the sequence of ITS1. Thus, the ability to differentiate amongst these strains of *L. procerum* is lost when ITS2 is used as the sole molecular marker. Sequence comparison of ITS1 would recover thirteen of the eighteen unique strains within the *L. wingfieldii*-*L. terebrantis*-*G. aurea* species complex, where as only eight strains would be identified based on sequence identity of ITS2. In addition, *G. aurea*

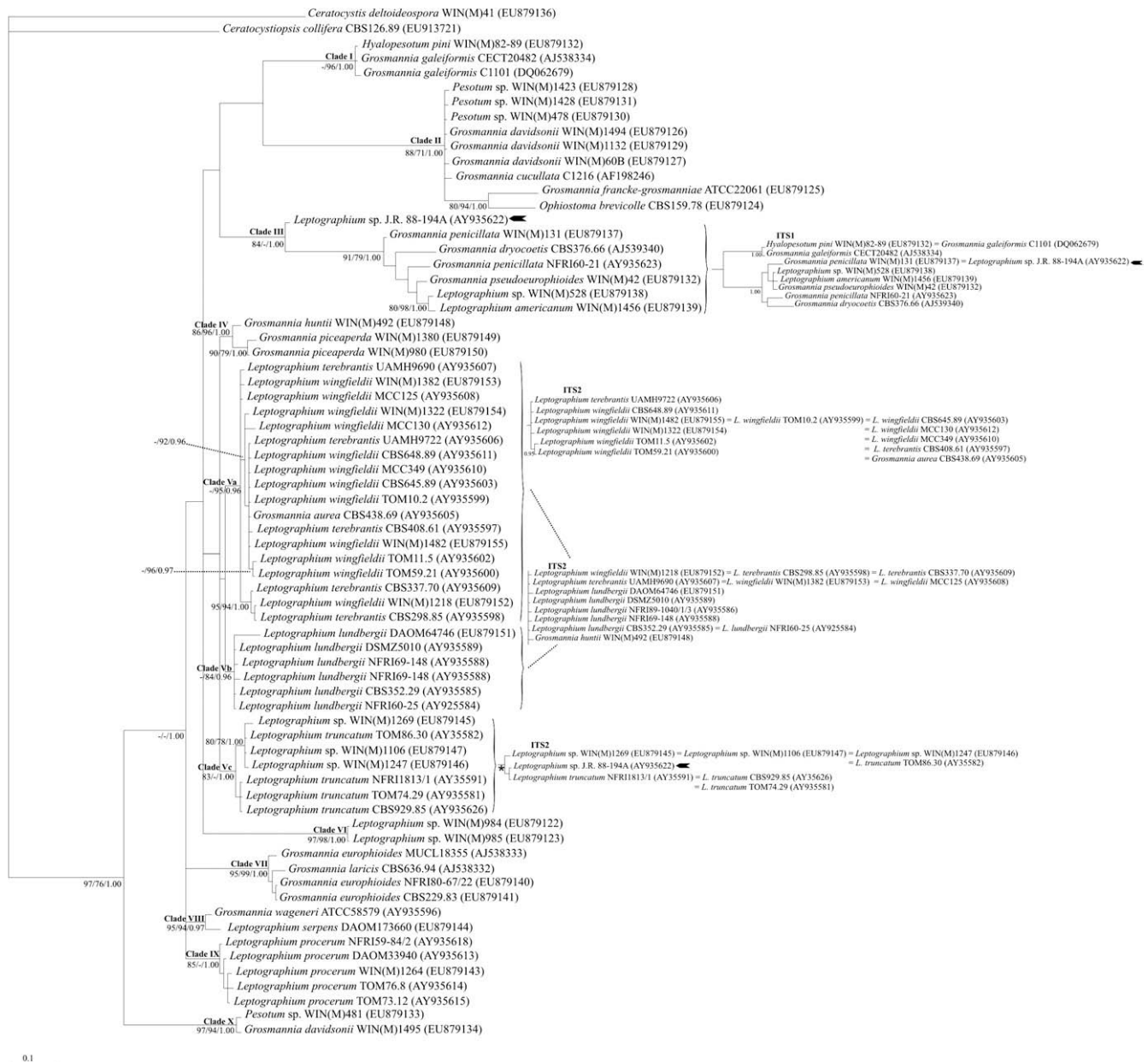


Fig. 3. Phylogenetic analysis of nuclear ITS1–5.8SrDNA–ITS2 DNA sequences in strains of *Grosmannia*, *Leptographium*, and related fungal taxa. Branch lengths were determined using the Bayesian consensus outfile. For Bayesian analysis, the TVM + I + G model (based on AIC) was selected. Values at the nodes were determined using algorithms in DNA PARS/Tree Puzzle/Mr. Bayes programs. “–” indicates the node is absent or the posterior probability or bootstrap value is not well supported (a posterior probability value of less than 0.95 for Bayesian analysis and bootstrap values less than 70% for parsimony and maximum likelihood analyses). The parsimony analysis combined with bootstrap analysis as performed by the TNT program (Tree analysis using New Technology; <http://www.zmuc.dk/public/Phylogeny/TNT/>) generated a tree topology essentially identically that that obtained from DNAPARS analysis. The major clades are indicated in roman numerals. Based on morphological criteria and molecular data *Ophiostoma brevicolle* should be included within the genus *Grosmannia* Goid. (Hausner et al., 1993b; Zipfel et al., 2006). *Leptographium* sp. strain J.R. 88-194A is marked by the black arrow; its position varies depending of which segment of the ITS region is used as the phylogenetic marker.

strain CBS438.89, a strain with a known teleomorphic (sexual) state would be indistinguishable from the anamorphic (asexual) *Leptographium* strains based on its ITS2 sequence. These results indicate that the distinction between strains and species of *Leptographium*/*Grosmannia* is better represented by sequence analyses that incorporate the entire ITS–5.8S region. Moreover the ITS phylogenetic analysis does confirm that *Leptographium* species represent mitotic derivatives of *Grosmannia* species (Zipfel et al., 2006).

An extreme example of distinct strains sharing identical ITS segments is represented by the *Leptographium* strain J.R. 88-194A [=WIN(M)1376, Hausner et al., 2005]: sequence identity of ITS1 between *Leptographium* strain J.R. 88-194A and *G. penicillata* strain

WIN(M)131 is 100%, while the sequence identity of ITS2 between *Leptographium* strain J.R. 88-194A and *L. truncatum* strains NFR18-13/1, TOM74.29 [=WIN(M)1246; AY935181; see Fig. 3], and CBS929.85 is 99%. Unlike the examples described in the previous section, phylogenetic analysis of the ITS–5.8S region indicates that these strains do not share a recent common ancestor (Fig. 3). Consequently, the phylogenetic position of *Leptographium* strain J.R. 88-194A (identified by the black arrow in Fig. 3 and Supplementary Figs. 1 and 2) appears to be unstable, as it depends on the particular segment within the ITS region that is subjected to phylogenetic analysis. When ITS1 alone, or the entire ITS region is analyzed, *Leptographium* strain J.R. 88-194A and *G. penicillata*

strain WIN(M)131 are grouped in the same clade (clade III in Fig. 3). However, analysis based on just the ITS2 segment places *Leptographium* strain J.R. 88-194A in clade Vc, with strains of *L. truncatum*. A similar phenomenon has been recently observed between fungal isolates of *Ceratobasidium oryzae-sativae* and *Thanatephorus cucumeris* (Xie et al., 2008). In the study the authors suggest the possibility of a rare intergeneric hybridization event that may have allowed for a mitotic genetic recombination event that generated biological chimeric ITS forms, but the mechanism behind this phenomenon was not described. One could assume it involved rare hyphal fusion between two different fungal species that allowed for the transfer of nuclei. This could have eventually led to the fusion of nuclei between two different species and mitotic recombination, a situation analogous to a parasexual cycle (Tinline and MacNeill, 1969; Croll et al., 2009).

3.5. Possible constraints involved in conservation of RNA structure

For detailed structural analyses of the major helix of ITS1 and helices I-IV of ITS2, we selected ten strains to highlight unusual sequence/structural features: one of these strains was *Pesotum* sp. strain WIN(M)481, which of the ingroup sequences is the most distantly related to the remaining sequences in the data set, was selected as the reference strain from which structural comparisons were made.

Based on the RNA modeling the following observations were made: (1) Variability in the length of the major helix of ITS1 can be the result of insertions, deletions, and possible RNA strand slippage events (Figs. 1 and 4a). (2) CBCs and hemi-CBCs maintain helical structure in ITS segments and also support our proposed models for the major hairpin stem in ITS1. (3) Insertions and deletions are accommodated via compensating indels on the opposite side of the helix and/or by potential slippage of the RNA strand to reform the helix (Fig. 4). The terminal hairpin loop of ITS1 is a hotspot for slippage events: its size contracts and expands, and nucleotides from the 3' side of the helix may potentially slide over the top loop and position themselves on the 5' side to base pair with neighbouring nucleotides (Fig. 4a). Moreover, strand slippage appears to be more common on the 3' side of the major helix. Near the base of the helix, deletions are typically compensatory on both sides of the hairpin, whereas at the top insertions and deletions (as well as substitutions in some sequences) may also be accommodated by potential RNA strand slippage.

A noteworthy exception to the observation of compensatory/slippage events balancing indels was found in the unusually short ITS1 sequence of *L. procerum* strain NFRI59-84/2. As described above, there is a deletion of 22 nt on the 3' side of the major helix near its midpoint but there is no compensating deletion on the 5' side; these unpaired nucleotides may interact with each other to form a short lateral helix (Fig. 4a).

The extended hairpin in ITS1 contains a plethora of so-called mutually informative sites; that is, sites which are involved in base pairing in the absence of nucleotide conservation. As shown in Fig. 1b, mutually informative sites are found at the base of the major helix in the GA/CT stretch, near the midpoint where there are polyGCs on both sides of the helix, and in the G-rich region on the 3' side of the hairpin, near the tip. The proximal region of the helix also contains numerous sites with CBCs and hemi-CBCs.

In ITS2, mutually informative sites were identified in all four helices (Fig. 2b). The final two nucleotides (positions 118–119) of helix II are dynamic sites; G–T transversion of the penultimate nucleotide in the stem is potentially accompanied by slippage of the RNA strand in the central loop into helix II to base pair with the first G (position 39). In helix III, the nucleotides on the 5' side of the stem are more conserved than those on the opposing side of the stem. The 3' terminal is the most variable region of the stem

and is one of the main sites of possible strand slippage events that result in expansion or contraction of both helix IV and the unpaired nucleotides in the loop between helices III and IV.

4. Discussion

4.1. Mechanisms involved in the conservation of the RNA secondary structures of ITS segments

One goal of this study was to identify the potential effects on RNA secondary structure of CBCs, hemi-CBCs, and indels. For the purpose of identifying potential RNA structural constraints that may influence the evolution of ITS sequences, we posed the following questions: (1) What are the effects on the RNA secondary structure of nucleotide substitutions and indels at the DNA level? (2) Do sequence changes disrupt base pairing (and to what extent) or are there compensatory changes to maintain the overall structure (compensating indels, CBCs, hemi-CBCs, or possible RNA strand slippage that restore hairpin structures)? Analysis of variations in the DNA sequence and RNA secondary structure may be useful for elucidating the evolutionary pressures on ITS segments.

Mono and di-nucleotide repeats are viewed as potential markers for replication slippage (Levinson and Gutman, 1987), particularly if the duplication or deletion events occurred 5' to the existing repeat. Analysis of the sequence alignment for each ITS sequence (excluding the phylogenetic outgroups) with the Weblogo program (Crooks et al., 2004) revealed conserved motifs of several long G and C mononucleotide repeats, suggesting that replication slippage may be an important mechanism for generating ITS sequence diversity. It has been shown that in variable regions of the SSU gene replication slippage occurs frequently (Hancock and Dover, 1990; Hancock and Vogler, 2000). It was noted that within the SSU rDNA indels generated by slippage frequently result in compensatory events (compensatory slippage or point mutations) that allow RNA secondary structures to be maintained. It appears that we observed similar consequences for slippage-derived sequences within ITS1 and ITS2. This raises an important issue, as it has been suggested that slippage-derived sequences tend to be self-complementary and, thus, at the RNA level stem-loop structures could be self-organizing as a consequence of random replication slippage events and point mutations (Hancock and Vogler, 2000). There is the potential risk that similar ITS RNA structures are observed in a wide range of organisms due to convergent evolution; that is, the structures are the result of the underlying mutational mechanisms outlined above and not necessarily due to functional constraints.

4.2. GC balance between ITS1 and ITS2

Previously, Hausner and Wang (2005) suggested that molecular co-evolution exists between ITS1 and ITS2 with respect to the length of these sequence elements, although no strong functional basis for this observation was proposed. Intraspecific ITS variability within the fungi was recently assessed by Nilsson et al. (2008) and they noted that variation in the ITS1 and ITS2 regions were highly correlated, suggesting the two regions do not evolve independently. Torres et al. (1990) observed that amongst many eukaryotes a GC balance appears to exist between ITS1 and ITS2 such that the GC content of ITS1 is nearly identical to that of ITS2, irrespective of the GC content of the corresponding 5.8S gene. This phenomenon has been observed in many plants (Jobst et al., 1998) and we also observed in our fungal ITS sequences a GC balance and GC bias in the rDNA ITS sequences compared to the 5.8S gene sequence. The ITS2 sequences in our fungal strains were unusually GC-rich compared to green algal strains belonging to

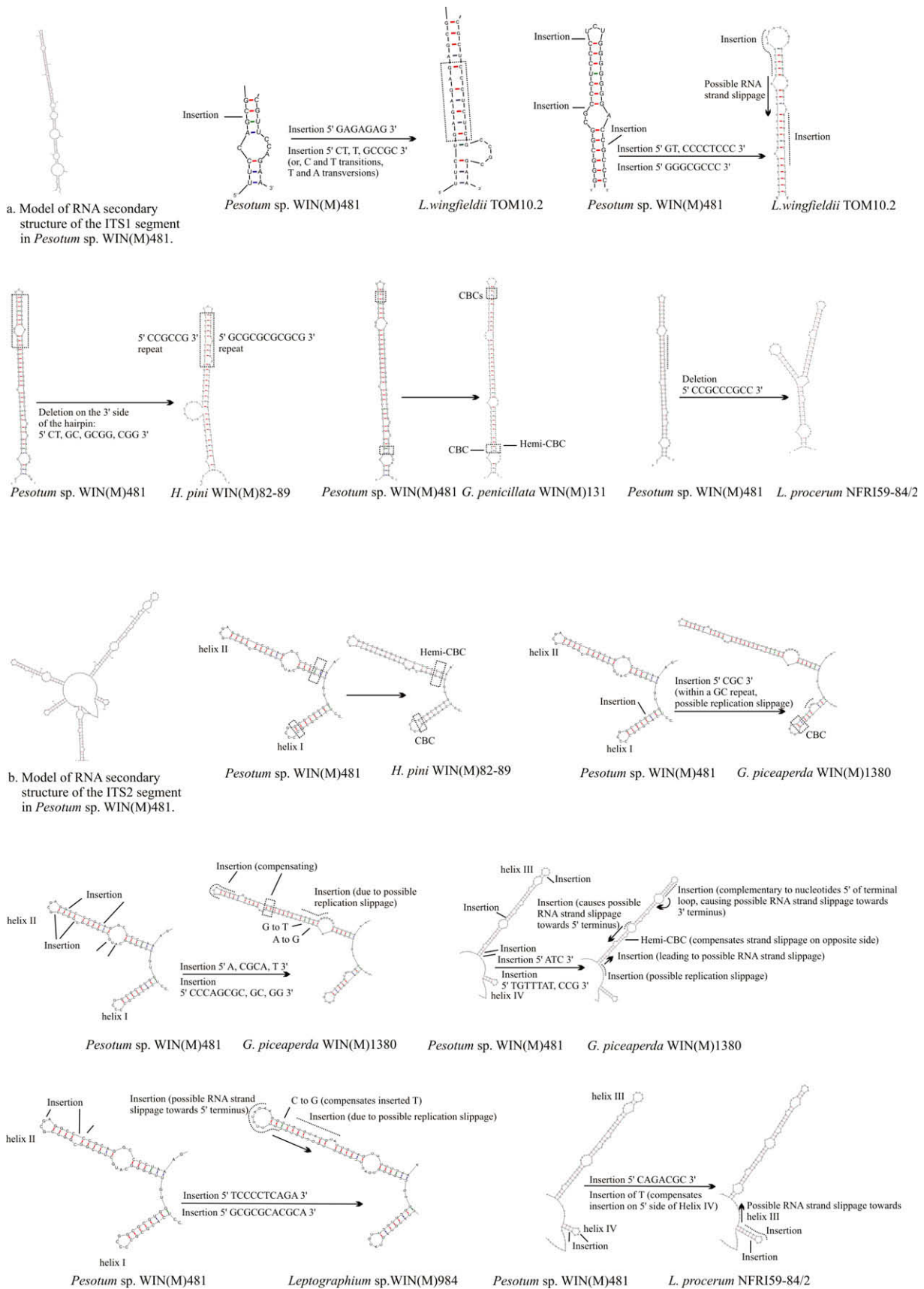


Fig. 4. Variability in the length of the major helix of ITS1 is caused by insertions, deletions, and putative RNA strand slippage (a). Helical regions may be maintained by compensating indels, CBCs, hemi-CBCs, and possible slippage of the RNA strand. The 5' and 3' sides of the hairpin at the proximal and distal sections are potential hotspots for expansion/contraction of sequence motifs. Substitution, insertion, and deletion events in helices I–IV of ITS2 may be accommodated by compensatory and slippage events that maintain RNA secondary structure (b). The 3' terminus at the base of helix III is hypervariable and is one of the main sites of potential RNA strand slippage. Helix IV is variable in length and sequence and variation is influenced by RNA strand slippage events occurring in helix III and in the single-stranded junction between helices III and IV.

the Volvocales, whose mol% GC ranges from 35.7 for *Pleodorina japonica* to 58.6 for *Chlamydomonas callosa* (Mai and Coleman, 1997). The size and GC contents of both ITS regions in our strains are comparable to those described by Nazar et al. (1987) for the thermophilic fungus *Thermomyces lanuginosus*. In this species, the length of ITS1 is 208 nt and its G + C content is 65.4%, and the size of ITS2 is 170 nt, with a G + C value of 68.2%. The authors attributed the unusually high GC content as an adaptation to the elevated temperature of the environment. Within the ITS region of the powdery mildews (Ascomycota, Erysiphaceae) a GC balance was observed between the two ITS regions and a positive correlation was noted between G + C content and ITS length, however, no explanations could be provided (Takamatsu et al., 1998). A GC balance between ITS1 and ITS2 (71.84% and 73.25%, respectively) was also documented in species of cacti belonging to the genus *Mammillaria*, family *Cactaceae* (Harpke and Peterson, 2006). The fungal strains examined in this work originate from the Northern Hemisphere and temperate zones and are mesophilic, growing poorly at temperatures above 25 °C (Upadhyay, 1981). Thus, it is likely that the high GC content is not an adaptation to environmental temperature in the fungal strains examined here, and there may be an alternative or additional evolutionary pressure behind the high GC content.

It is not apparent what types of mechanisms would promote the molecular co-evolution that has been noted within the fungal ITS1 and ITS2 segments in terms of length and GC balance, however, structural constraints might set the limits on how ITS sequences evolve. Data from both biochemical studies and comparative sequence analyses of the ITS regions indicate that ITS RNA transcripts form extended helical structures, which is essential to their biological function (Lalev and Nazar, 1999; Côté and Peculis, 2001; Mai and Coleman, 1997; Schultz et al., 2005; Wolf et al., 2005; Keller et al., 2009). The ITS1 region appears to act as a “biological spring” to bring into close proximity the appropriate termini of 18S, 5.8S, and ITS segments during processing of the pre-RNA precursor (Nazar et al., 1987; Lalev and Nazar, 1998), and this functional constraint may provide sufficient evolutionary pressure to conserve base pairing interactions. GC-rich segments may have a role in forming and/or stabilizing the extensive base pairing of helical regions in the RNA secondary structure such as the central extended hairpin of ITS1 and the 3–4 helices radiating from the “palm” structural model for ITS2 (Mai and Coleman, 1997; Schultz et al., 2005; Wolf et al., 2005) and the base pairing between the 5' terminus of ITS2 and the 3' terminus of the LSU (Lalev and Nazar, 1999). These observations suggest that the preservation of RNA secondary and/or tertiary structure, and, ultimately biological function, is a major constraint acting on the evolution of ITS sequences.

Future efforts in elucidating the mechanisms that allow for evolutionary changes and constraints that limit change and possible interdependence of ITS1 and ITS2 sequences amongst the fungi would benefit from comparative sequence analysis of ITS regions from other fungal groups such as the well characterized members of the genus *Saccharomyces*.

4.3. The use of the ITS region as a phylogenetic marker

A second objective of this study was to assess both the level of branch support and effects on tree topology obtained from the phylogenetic analysis of each segment individually and of the entire region, including the highly-conserved 5.8S region that is situated between ITS1 and ITS2. The latter goal stems from the wide-spread application of the ITS region as a marker in phylogenetic and taxonomic studies. It was observed that the number of strains that could be distinguished using ITS1 sequences was greater than when ITS2 sequences were used (compare Supplementary Figs. 1 and 2) and analysis of just the latter region (i.e. excluding

ITS1 and 5.8S sequences) resulted in phylogenetic trees with numerous unresolved polytomies. Within the *Hypocreales*, specifically the *Gibberella fujikuroi* complex, the ITS regions, when analyzed individually, performed poorly and again the ITS2 segment was noted to be less informative when compared to the ITS1 region (Lieckfeldt and Seifert, 2000).

Amongst the eukaryotes, ITS regions vary greatly in size and sequence (reviewed in Hausner and Wang, 2005). The analysis of ITS sequences, including the use of RNA secondary structural features to guide the alignment of ambiguous regions, has become an important tool in phylogenetic analyses (Coleman, 2003, 2007, 2009; Goertzen et al., 2003; Young and Coleman, 2004; Won and Renner, 2005; Schultz et al., 2006; Aguilar and Sánchez, 2007; Müller et al., 2007; Krüger and Gargas, 2008; Ryberg et al., 2008; Seibel et al., 2008; Wolf et al., 2008; Schultz and Wolf, 2009). One caveat to the wide-spread application of ITS segments in phylogenetic and taxonomic studies is the potential influence on the rate and types of nucleotide changes arising from the possible co-evolution of the two spacer regions and compensatory slippage (interdependence of sites). These are problematic, as phylogenetic algorithms assume that every nucleotide position evolves independently. Previous studies show that the ITS RNA structures might be more conserved than the actual nucleotide sequences (Joseph et al., 1999; Gottschling and Plötner, 2004; Schultz et al., 2005; Hausner and Wang, 2005), suggesting a functional constraint, connected with the RNA fold, is influencing the evolution of these sequences. While convergence and other factors do not strictly affect the use of ITS sequences in barcoding studies, the utility of the ITS region for developing probes to rapidly identify organisms (El Karkouri et al., 2007; Landis and Gargas, 2007) may be affected by our observation that the ITS2 segment is more conserved than ITS1 in this group of ophiostomatoid fungi. Taxonomically distinct organisms may share identical ITS2 sequences, and the use of ITS2 alone could lead to erroneous identification of unknown strains.

The observation that replication slippage may promote compensatory events that maintain thermodynamically favorable RNA folds (either due to convergent evolution or functional constraints) may pose difficulties regarding the use of secondary structure in improving ITS sequence alignments. Positional homology of a nucleotide within the primary sequence may not correspond to the placement of this base within an RNA fold. Slippage of the RNA strand to compensate for an event at the primary sequence level (due to indels, for example) could move a base into a different structural location from its original position in the RNA fold. Alignments guided by structural criteria may essentially align non-homologous positions (positions that happen to occupy the same “site” within a fold but do not share a common ancestral sequence). It might be more beneficial to analyze alignments for evidence of positions that are prone to or the result of replication slippage events. Compensatory mutations may then be more readily recognized and down-weighted in phylogenetic analyses. Although other genes, such as *COI* (Seifert et al., 2007) or *ND6* (Santamaria et al., 2009) along with rRNA-coding genes may be used in the future for DNA barcoding studies, the utility of the multicopy rDNA sequences, with regards to PCR primer design and amplification, will ensure the continued use of ITS sequences for phylogenetic studies. This in particular applies to situations in which only limited amounts of DNA can be recovered, such as studies with herbarium specimens or environmental samples. Gaining a better understanding of the mode of fungal ITS sequence evolution, the nature of the GC bias, and the constraints on the ITS sequences may assist in developing improved evolutionary models for phylogenetic analysis using ITS sequences. Finally, this work highlights the mechanisms that maintain the pan-eukaryotic ITS2 structure (Coleman, 2007) and the hairpin type structures commonly observed the fungal ITS1 region.

Acknowledgments

The authors gratefully acknowledge funding for this research in part through an operating grant from the Natural Sciences and Engineering Research Council of Canada (NSERC) to G.H. and graduate studentships/scholarships to T.M (NSERC Postgraduate Scholarship M award, 2004–2006; University of Manitoba Graduate Fellowship, 2006–2007; Manitoba Health Research Council, 2007–2008). The authors express sincere gratitude to Dr. James Reid (Department of Microbiology, University of Manitoba) for generously supplying strains for this study, Dr. Mahmood Iranpour (Department of Microbiology, University of Manitoba) for providing unpublished sequences, Tamara Corkery (Department of Microbiology, University of Manitoba) for contributions to isolation and purification of DNA and generating sequence data, Shelly Rudski (Department of Microbiology, University of Manitoba) for contributions to the generation of sequence data, David Boguski (Department of Biological Sciences, University of Manitoba) for suggestions with phylogenetic analyses, and to anonymous reviewers for their helpful suggestions.

Appendix A. Supplementary material

Supplementary data associated with this article can be found, in the online version, at doi:10.1016/j.fgb.2009.08.001.

References

- Abeyrathne, P.D., Lavlev, A.I., Nazar, R.N., 2002. A RAC protein-binding site in the internal transcribed spacer 2 of Pre-rRNA transcripts from *Schizosaccharomyces pombe*. *J. Biol. Chem.* 277, 21291–21299.
- Aguilar, C., Sánchez, J.A., 2007. Phylogenetic hypotheses of gorgoniid octocorals according to ITS2 and their predicted RNA secondary structures. *Mol. Phylogenet. Evol.* 43, 774–786.
- Buchan, A., Newell, S.Y., Moreta, J.I., Moran, M.A., 2002. Analysis of internal transcribed spacer (ITS) regions of rRNA genes in fungal communities in a Southeastern US salt marsh. *Micro. Ecol.* 43, 329–340.
- Clark, C.G., 1987. On the evolution of ribosomal RNA. *J. Mol. Evol.* 25, 343–350.
- Coleman, A.W., 2003. ITS2 is a double-edged tool for eukaryote evolutionary comparisons. *Trends Genet.* 19, 370–375.
- Coleman, A.W., 2007. Pan-eukaryote ITS2 homologies revealed by RNA secondary structure. *Nucleic Acids Res.* 35, 3322–3329.
- Coleman, A.W., 2009. Is there a molecular key to the level of “biological species” in eukaryotes? A DNA guide. *Mol. Phylogenet. Evol.* 50, 197–203.
- Côté, C.A., Peculis, B.A., 2001. Role of the ITS2-proximal stem and evidence for indirect recognition of processing sites in pre-rRNA processing in yeast. *Nucleic Acids Res.* 29, 2106–2116.
- Côté, C.A., Greer, C.L., Peculis, B.A., 2002. Dynamic conformational model for the role of ITS2 in pre-rRNA processing in yeast. *RNA* 8, 786–797.
- Croll, D., Giovannetti, M., Koch, A.M., Sbrana, C., Ehinger, M., Lammers, P.J., Sanders, I.R., 2009. Nonspecific vegetative fusion and genetic exchange in the arbuscular mycorrhizal fungus *Glomus intraradices*. *New Phytol.* 181, 924–937.
- Crooks, G.E., Hon, G., Chandonia, J.M., Brenner, S.E., 2004. Weblogo: a sequence logo generator. *Genome Res.* 14, 1188–1190.
- Druzhinina, I.S., Kopychinskiy, A.G., Komoń, M., Bissett, J., Szakacs, G., Kubicek, C.P., 2005. An oligonucleotide barcode for species identification in *Trichoderma* and *Hypocrea*. *Fungal Genet. Biol.* 42, 813–828.
- El Karkouri, K., Murat, C., Zampieri, E., Bonfante, P., 2007. Identification of internal transcribed spacer sequence motifs in truffles: a first step toward their DNA bar coding. *Appl. Environ. Microbiol.* 73, 5320–5330.
- Felsenstein, J., 2008. PHYLIP: Phylogeny Inference Package. Version 3.68. (Distributed by the author). Department of Genome Sciences and Department of Biology, University of Washington, Seattle, Wash. <<http://evolution.genetics.washington.edu/phylip/getme.html>>.
- Goertzen, L.R., Cannone, J.J., Gutell, R.R., Jansen, R.K., 2003. ITS secondary structure derived from comparative analysis: implications for sequence alignment and phylogeny of the Asteraceae. *Mol. Phylogenet. Evol.* 29, 216–234.
- Goloboff, P.A., Farris, J.S., Nixon, K.C., 2008. TNT, a free program for phylogenetic analysis. *Cladistics* 24, 774–786.
- Good, L., Intine, R.V., Nazar, R.N., 1997. Interdependence in the processing of ribosomal RNAs in *Schizosaccharomyces pombe*. *J. Mol. Biol.* 273, 782–788.
- Gorodkin, J., Heyer, L.J., Brunak, S., Stormo, G.D., 1997. Displaying the information contents of structural RNA alignments: the structure logos. *Comput. Appl. Biosci.* 13, 583–586.
- Gottschling, M., Plötner, J., 2004. Secondary structure models of the nuclear internal transcribed spacer regions and 5.8S rRNA in Calciodinelloideae (Peridiniaceae) and other dinoflagellates. *Nucleic Acids Res.* 32, 307–315.
- Hancock, J.M., Dover, G.A., 1990. ‘Compensatory slippage’ in the evolution of ribosomal RNA genes. *Nucleic Acids Res.* 18, 5949–5954.
- Hancock, J.M., Vogler, A.P., 2000. How slippage-derived sequences are incorporated into rRNA variable-region secondary structure: implications for phylogeny reconstruction. *Mol. Phylogenet. Evol.* 14, 366–374.
- Harpke, D., Peterson, A., 2006. Non-concerted ITS evolution in *Mammillaria* (Cactaceae). *Mol. Phylogenet. Evol.* 41, 579–593.
- Harrington, T.C., 1993. Biology and taxonomy of fungi associated with bark beetles. In: Schowalter, T.D., Filip, G.M. (Eds.), *Beetle-Pathogen Interactions in Conifer Forests*. Academic Press, pp. 37–58.
- Hasegawa, M., Kishino, H., Yano, T., 1985. Dating of the human-ape splitting by a molecular clock of mitochondrial DNA. *J. Mol. Evol.* 22, 160–174.
- Hausner, G., Wang, X., 2005. Unusual compact rDNA gene arrangements within some members of the Ascomycota: evidence for molecular co-evolution between ITS1 and ITS2. *Genome* 48, 648–660.
- Hausner, G., Reid, J., Klassen, G.R., 1992. Do galeate-ascospore members of the *Cephalosporaceae*, *Endomycetaceae* and *Ophiostomataceae* share a common phylogeny? *Mycologia* 84, 870–881.
- Hausner, G., Klassen, G.R., Reid, J., 1993a. Unusually compact ribosomal RNA gene cluster in *Sphaeronaemella fimicola*. *Curr. Genet.* 23, 357–359.
- Hausner, G., Reid, J., Klassen, G.R., 1993b. On the phylogeny of *Ophiostoma*, *Ceratocystis* s.s., *Microascus*, and relationships within *Ophiostoma* based on partial ribosomal DNA sequences. *Can. J. Bot.* 71, 1249–1265.
- Hausner, G., Iranpour, M., Kim, J.-J., Breuil, C., Davis, C.N., Gibb, E.A., Reid, J., Loewen, P.C., Hopkin, A.A., 2005. Fungi vectored by the introduced bark beetle *Tomicus piniperda* in Ontario, Canada and comments on the taxonomy of *Leptographium lundbergii*, *L. terebrantis*, *L. truncatum* and *L. wingfieldii*. *Can. J. Bot.* 83, 1222–1237.
- Hershkovitz, M.A., Zimmer, E.A., Hans, W.J., 1999. Ribosomal DNA sequences and angiosperm systematics. In: Hollingsworth, P.M., Bateman, R.M., Gornall, R.J. (Eds.), *Molecular Systematics and Plant Evolution*. Taylor and Francis, London, pp. 268–326.
- Hibbett, D.S., Binder, M., Bischoff, J.F., Blackwell, M., Cannon, P.F., Eriksson, O.E., Huhndorf, S., James, T., Kirk, P.M., Lücking, R., Thorsten Lumbsch, H., Lutzoni, F., Matheny, P.B., McLaughlin, D.J., Powell, M.J., Redhead, S., Schoch, C.L., Spatafora, J.W., Stalpers, J.A., Vilgalys, R., Aime, M.C., Aptroot, A., Bauer, R., Begerow, D., Benny, G.L., Castlebury, L.A., Crous, P.W., Dai, Y.C., Gams, W., Geiser, D.M., Griffith, G.W., Gueidan, C., Hawksworth, D.L., Hestmark, G., Hosaka, K., Humber, R.A., Hyde, K.D., Ironside, J.E., Kõljalg, U., Kurtzman, C.P., Larsson, K.H., Lichtwardt, R., Longcore, J., Miadlikowska, J., Miller, A., Moncalvo, J.M., Mozley-Standridge, S., Oberwinkler, F., Parmasto, E., Reeb, V., Rogers, J.D., Roux, C., Ryvarden, L., Sampaio, J.P., Schüssler, A., Sugiyama, J., Thorn, R.G., Tibell, L., Untereiner, W.A., Walker, C., Wang, Z., Weir, A., Weiss, M., White, M.M., Winka, K., Yao, Y.J., Zhang, N., 2007. A higher-level phylogenetic classification of the fungi. *Mycol. Res.* 111, 509–547.
- Horton, T.R., 2002. Molecular approaches to ectomycorrhizal diversity studies: variations in ITS at a local scale. *Plant Soil* 244, 29–39.
- Jacobs, K., Wingfield, M.J., Wingfield, B.D., 2001. Phylogenetic relationships in *Leptographium* based on morphological and molecular characters. *Can. J. Bot.* 79, 719–732.
- Jobst, J., King, K., Hemleben, V., 1998. Molecular evolution of the internal transcribed spacers (ITS1 and ITS2) and phylogenetic relationships among species of the family Cucurbitaceae. *Mol. Phylogenet. Evol.* 9, 204–219.
- Joseph, N., Krauskopf, E., Vera, M.I., Michot, B., 1999. Ribosomal internal transcribed spacer 2 (ITS2) exhibits a common core of secondary structure in vertebrates and yeast. *Nucleic Acids Res.* 27, 4533–4540.
- Keller, A., Schleicher, T., Schultz, J., Müller, T., Dandekar, T., Wolf, M., 2009. 5.8S-28S rRNA interaction and HMM-based ITS2 annotation. *Gene* 430, 50–57.
- Kennedy, N., Clipson, N., 2003. Fingerprinting the fungal community. *Mycologist* 17, 158–164.
- Krüger, D., Gargas, A., 2008. Secondary structure of ITS2 rRNA provides taxonomic characters for systematic studies – a case in Lycopodiaceae (Basidiomycota). *Mycol. Res.* 112, 316–330.
- Lalev, A.I., Nazar, R.N., 1998. Conserved core structure in the internal transcribed spacer 1 of the *Schizosaccharomyces pombe* precursor ribosomal RNA. *J. Mol. Biol.* 284, 1341–1351.
- Lalev, A.I., Nazar, R.N., 1999. Structural equivalence in the transcribed spacers of pre-rRNA transcripts in *Schizosaccharomyces pombe*. *Nucleic Acids Res.* 27, 3071–3078.
- Lalev, A.I., Nazar, R.N., 2001. A chaperone for ribosome maturation. *J. Biol. Chem.* 276, 16655–16659.
- Lalev, A.I., Abeyrathne, P.D., Nazar, R.N., 2000. Ribosomal RNA maturation in *Schizosaccharomyces pombe* is dependent on a large ribonucleoprotein complex of the internal transcribed spacer 1. *J. Mol. Biol.* 302, 65–77.
- Landis, F.C., Gargas, A., 2007. Using ITS2 secondary structure to create oligonucleotide probes for fungi. *Mycologia* 99, 681–692.
- Levinson, G., Gutman, G.A., 1987. Slipped-strand mispairing: a major mechanism for DNA sequence evolution. *Mol. Biol. Evol.* 4, 203–221.
- Lieckfeldt, E., Seifert, K.A., 2000. An evaluation of the use of ITS sequences in the taxonomy of the Hypocreales. *Stud. Mycol.* 45, 35–44.
- Mai, J.C., Coleman, A.W., 1997. The internal transcribed spacer 2 exhibits a common secondary structure in green algae and flowering plants. *J. Mol. Evol.* 44, 258–271.
- Mathews, D.H., Sabina, J., Zuker, M., Turner, D.H., 1999. Expanded sequence dependence of thermodynamic parameters improves prediction of RNA secondary structure. *J. Mol. Biol.* 288, 911–940.

- Meyer, I.M., Miklós, I., 2007. SimulFold: simultaneously inferring RNA structures including pseudoknots, alignments, and trees using a Bayesian MCMC framework. *PLoS Comput. Biol.* 3, e149.
- Mitchell, J.I., Zuccaro, A., 2006. Sequences, the environment and fungi. *Mycologist* 20, 62–74.
- Müller, T., Philippi, N., Dandekar, T., Schultz, J., Wolf, M., 2007. Distinguishing species. *RNA* 13, 1469–1472.
- Nazar, R.N., 1980. A 5.8S rRNA-like sequence in prokaryotic 23S rRNA. *FEBS Lett.* 119, 212–214.
- Nazar, R.N., 2003. Ribosome biogenesis in yeast: rRNA processing and quality control. In: Arora, D.K., Khachatourians, G.G. (Eds.), *Applied Mycology and Biotechnology, Fungal Genomics and Bioinformatics*, vol. 3. Elsevier Inc. Science & Technology/Academic Press, San Diego, Calif, pp. 161–183.
- Nazar, R.N., 2004. Ribosomal RNA processing and ribosome biogenesis in eukaryotes. *IUBMB Life* 56, 457–465.
- Nazar, R.N., Wong, W.M., Abrahamson, J.L.A., 1987. Nucleotide sequence of the 18–25S ribosomal RNA intergenic region from a thermophile, *Thermomyces lanuginosus*. *J. Biol. Chem.* 262, 7523–7527.
- Nicholas, K.B., Nicholas Jr., H.B., Deerfield II, D.W., 1997. GeneDoc: analysis and visualization of genetic variation. *EMBNEW.NEWS* 4, 14.
- Nilsson, R.H., Kristiansson, E., Ryberg, M., Hallenberg, N., Larsson, K.H., 2008. Intraspecific ITS variability in the kingdom fungi as expressed in the international sequence databases and its implications for molecular species identification. *Evol. Bioinfo.* 4, 193–201.
- Nilsson, R.H., Bok, G., Ryberg, M., Kristiansson, E., Hallenberg, N., 2009. A software pipeline for processing and identification of fungal ITS sequences. *Source Code Biol. Med.* 4, 1.
- Page, R.D., 1996. TREEVIEW: an application to display phylogenetic trees on personal computers. *Comput. Appl. Biosci.* 12, 357–358.
- Piercey-Normore, M.D., Coxson, D., Goward, T., Goffinet, B., 2006. Phylogenetic position of a Pacific Northwest North American endemic cyanolichen, *Nephroma occultum* (Ascomycota, *Peltigerales*). *The Lichenologist* 38, 441–456.
- Posada, D., Crandall, K.A., 1998. MODELTEST: testing the model of DNA substitution. *Bioinformatics* 14, 817–818.
- Ranjard, L., Poly, F., Lata, J.C., Mougél, C., Thioulouse, J., Nazaret, S., 2001. Characterization of bacterial and fungal soil communities by automated ribosomal intergenic spacer analysis fingerprints: biological and methodological variability. *Appl. Environ. Microbiol.* 67, 4479–4487.
- Ronquist, F., Huelsenbeck, J.P., 2003. MrBayes 3: Bayesian phylogenetic inference under mixed models. *Bioinformatics* 19, 1572–1574.
- Ryberg, M., Nilsson, R.H., Kristiansson, E., Töpel, M., Jacobsson, S., Larsson, E., 2008. Mining metadata from unidentified ITS sequences in GenBank: a case study in *Inocybe* (Basidiomycota). *BMC Evol. Biol.* 8, 50.
- Santamaria, M., Vicario, S., Pappadà, G., Scioscia, G., Scazzocchio, C., Saccone, C., 2009. Towards barcode markers in Fungi: an intron map of Ascomycota mitochondria. *BMC Bioinformatics* 10 (Suppl. 6), S15.
- Schmidt, H.A., Strimmer, K., Vingron, M., von Haeseler, A., 2002. TREE-PUZZLE: maximum likelihood phylogenetic analysis using quartets and parallel computing. *Bioinformatics* 18, 502–504.
- Schneider, T.D., Stephens, R.M., 1990. Sequence logos: a new way to display consensus sequences. *Nucleic Acids Res.* 18, 6097–6100.
- Schultz, J., Wolf, M., 2009. ITS2 sequence-structure analysis in phylogenetics: a how-to manual for molecular systematics. *Mol. Phylogenet. Evol.* 52, 520–523.
- Schultz, J., Maisel, S., Gerlach, D., Müller, T., Wolf, M., 2005. A common core of secondary structure of the internal transcribed spacer 2 (ITS2) throughout the Eukaryota. *RNA* 11, 361–364.
- Schultz, J., Müller, T., Achtziger, M., Seibel, P.N., Dandekar, T., Wolf, M., 2006. The internal transcribed spacer 2 database—a web server for (not only) low level phylogenetic analyses. *Nucleic Acids Res.* 34, W704–W707.
- Seibel, P.N., Müller, T., Dandekar, T., Wolf, M., 2008. Synchronous visual analysis and editing of RNA sequence and secondary structure alignments using 4SALE. *BMC Res. Notes* 1, 91.
- Seifert, K.A., Samson, R.A., Dewaard, J.R., Houbraken, J., Lévesque, C.A., Moncalvo, J.M., Louis-Seize, G., Hebert, P.D., 2007. Prospects for fungus identification using CO1 DNA barcodes, with *Penicillium* as a test case. *Proc. Natl. Acad. Sci.* 104, 3901–3906.
- Selig, C., Wolf, M., Müller, T., Dandekar, T., Schultz, J., 2008. The ITS2 Database II: homology modelling RNA structure for molecular systematics. *Nucleic Acids Res.* 36, D377–380.
- Swofford, D.L., 2002. PAUP*. Phylogenetic analysis using parsimony (* and other methods). Version 4. Massachusetts: Sinauer Associates.
- Takamatsu, S., Hirata, T., Sato, Y., 1998. Phylogenetic analysis and predicted secondary structures of the rDNA internal transcribed spacers of the powdery mildew fungi (Erysiphaceae). *Mycoscience* 39, 441–453.
- Tinline, R.D., MacNeill, B.H., 1969. Parasexuality in plant pathogenic fungi. *Annu. Rev. Phytopathol.* 7, 147–168.
- Torres, R.A., Ganal, M., Hemleben, V., 1990. GC balance in the internal transcribed spacers ITS 1 and ITS 2 of nuclear ribosomal RNA genes. *J. Mol. Evol.* 30, 170–181.
- Upadhyay, H.P., 1981. Monograph of *Ceratocystis* and *Ceratocystiopsis*. University of Georgia Press, GA.
- Wolf, M., Achtziger, M., Schultz, J., Dandekar, T., Müller, T., 2005. Homology modeling revealed more than 20,000 rRNA internal transcribed spacer 2 (ITS2) secondary structure. *RNA* 11, 1616–1623.
- Wolf, M., Ruderisch, B., Dandekar, T., Schultz, J., Müller, T., 2008. ProfDistS: (profile-) distance based phylogeny on sequence-structure alignments. *Bioinformatics* 24, 2401–2402.
- Won, H., Renner, S.S., 2005. The internal transcribed spacer of nuclear ribosomal DNA in the gymnosperm *Gnetum*. *Mol. Phylogenet. Evol.* 36, 581–597.
- Xia, X., 2000. *Data Analysis in Molecular Biology and Evolution*. Kluwer Academic Publishers.
- Xie, J., Fu, Y., Jiang, D., Li, G., Huang, J., Li, B., Hsiang, T., Peng, Y., 2008. Intergeneric transfer of ribosomal genes between two fungi. *BMC Evol. Biol.* 8, 87.
- Young, I., Coleman, A.W., 2004. The advantages of the ITS2 region of the nuclear rDNA cistron for analysis of phylogenetic relationships of insects: a *Drosophila* example. *Mol. Phylogenet. Evol.* 30, 236–242.
- Zhang, N., McCarthy, M.L., Smart, C.D., 2008. A macroarray system for the detection of fungal and oomycete pathogens of solanaceous crops. *Plant Dis.* 92, 953–960.
- Zipfel, R.D., de Beer, Z.W., Jacobs, K., Wingfield, B.D., Wingfield, M.J., 2006. Multi-gene phylogenies define *Ceratocystiopsis* and *Grosmannia* distinct from *Ophiostoma*. *Stud. Mycol.* 55, 75–97.
- Zuker, M., 2003. Mfold web server for nucleic acid folding and hybridization prediction. *Nucleic Acids Res.* 31, 3406–3415.